

The adsorption-desorption behavior of strontium ions with an impregnated resin containing di (2-ethylhexyl) phosphoric acid in aqueous solutions

Hossein Sid Kalal^{*}, Ali Reza Khanchi, Mojtaba Nejatlabaf,
Mohammad Reza Almasian, Kamal Saberyan and Mohammad Taghiof

*Materials and Nuclear Fuel Research School, Nuclear Science and Technology Research Institute, AEOI,
P.O. Box 11365-3486, Tehran, Iran*

(Received November 8, 2017, Revised January 27, 2018, Accepted January 29, 2018)

Abstract. An Amberlite XAD-4 resin impregnated with di(2-ethylhexyl)phosphoric acid was prepared and its adsorption-desorption behaviors with Sr(II) ions under various conditions was examined. The resin was characterized by fourier transform infrared and thermal analysis techniques. The effects contact time, temperature, pH, interfering ions and eluants were studied. Results showed that adsorption of Sr (II) well fitted with pseudo-second-order kinetic model. The equilibrium adsorption data of Sr (II) on the impregnated resin were analyzed by Jossens, Weber-van Vliet, Redlich-Peterson and Fritz-Schlunder models to find out desirable equilibrium condition. Among them, the Fritz-Schlunder model best fitted to the experimental data. The maximum sorption capacity of impregnated resin amounted to 0.45 mg/ g at pH 8.0 and 20°C.

Keywords: strontium removal; Amberlite XAD-4; di (2-ethylhexyl) phosphoric acid; isotherm study

1. Introduction

In recent years, a great effort has been focused on the control of heavy metals in surface and ground waters because of their toxic effects on human, animals and plants health. Strontium is one of the heavy metals which have dangerous health effect on human beings. Strontium has a similar biochemical behavior with calcium and can alter bone mineralization and cause bone deformities in the human body. Large amounts ingestion of strontium can develop into strontium rickets (Nielsen 2004, Greve *et al.* 2007, Prohl *et al.* 2006). Furthermore, among its isotopes; strontium-90 is one of the most dangerous materials which are produced from nuclear power plants with a relatively long half-life of about 28.8 years. Strontium-90 collects in the bone and bone marrow of humans and soft tissues, developing into anemia and leukemia (Grynpas *et al.* 1996). Several methods have been developed for the strontium separation from various samples until now. Some of these methods have been assigned to those involving the use of inorganic and hybrid ion exchangers (Taj *et al.* 2009, Xiusheu *et al.* 2008, Sivaih *et al.* 2005, Tripathi *et al.* 2003, Puziy

^{*}Corresponding author, Ph.D., E-mail: hsidkalal@aeoi.org.ir

1998, Cakir *et al.* 2014, Solecki *et al.* 2006, Biligin *et al.* 2001). The main drawback of these materials is that their reactions with some metal ions are irreversible and as a result, they are frequently not reusable and economical. Solvent extraction (Schulz *et al.* 1963, Kocherginsky *et al.* 2002, Dinga *et al.* 2010, Makrlik *et al.* 2010, Schulz 1968), ion exchange (Hafizi *et al.* 2011, Zhang *et al.* 1999), membrane (Ashraf Chaudry *et al.* 1994, Raut *et al.* 2012), combination of these methods (Jeong *et al.* 2002, Chen 2007) and extraction chromatography (Heilgeist 2000, Jyh-Herng *et al.* 2003) are other important methods. Of these methods, although the extraction chromatography is well-developed over the last twenty years, little attention has been paid to those particularly involving the reversible recovery of strontium.

The aim of this work was to study Sr (II) adsorption-desorption onto Amberlite XAD-4 resin impregnated with di (2-ethylhexyl) phosphoric acid (D2EHPA). To achieve this purpose, the effect of contact time, pH, initial concentration of Sr (II), temperature, interfering ions, thermodynamics and kinetics of adsorption were investigated.

2. Material and methods

2.1 Chemicals and reagents

All chemicals used were of analytical grade from Merck, Fluka and Sigma Aldrich companies. Standard and stock solutions were prepared using double distilled water. For further purification of the resin, it was washed with methanol, water, 1 mol/L HNO₃, water, 1 mol/L NaOH and water respectively. For adjusting the pH of solutions, we used 0.01-1M HCl and NaOH.

The pH of solutions was measured by a Metrohm instrument, model 744 pH meter (Zofingen, Switzerland). Infrared spectra were recorded by Vector 22 FT-IR spectrometer (Bruker, Germany) using the potassium bromide pellet method. The metal ion measurements were done using the Varian Turbo 150AX ICP-OES instrument. Thermal analysis was performed by Rheometric Scientific STA 1500H analyzer in argon atmosphere at a linear heating rate 10°C min⁻¹.

2.2 Conditioning of Amberlite XAD-4

We washed Amberlite XAD-4 resin with 4M HCl and then rinsed with water. Rinsing was continued until the pH of supernatant reached to neutral. After that, it was washed with a methanol-water (1:1) solution to remove residual monomer species and washed again with water. Then the resin was filtered and dried at room temperature for 24 hours and kept in a desiccator. Finally, it was stored in a polyethylene bottle.

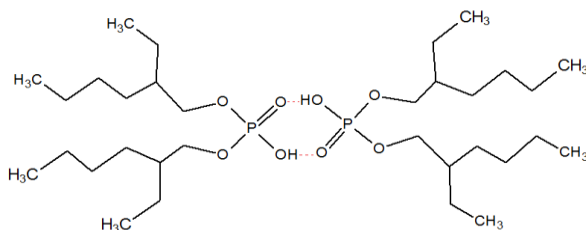


Fig. 1 Chemical structure of Di-(2-ethylhexyl) phosphoric acid (D2EHPA)

2.3 Impregnation procedure

The impregnated resin was prepared by mixing of 1g of purified Amberlite XAD-4 with 6ml of D2EHPA (Fig. 1) and 6ml of ethanol. The resulting slurry was gently stirred for 24 hrs. Then, ethanol was removed by evaporation at ambient temperature (25°C). Finally, the resin was dried at 50 °C.

2.4 Batch adsorption studies

Adsorption experiments were performed in various solutions by adding 0.1 or 0.2 g of the impregnated resins and 20 ml of Sr(II) ions with a concentration of 2.5 mg/L at 25±1°C during 5 hrs using a water bath shaker. The adsorbed metal ion q_e (mg/g) was calculated using the following equation

$$q_e = (C_0 - C_e) \times V / M \quad (1)$$

where C_0 and C_e are the initial and the equilibrium concentrations (mg/L) of metal ion in solution, respectively, V is the volume of solution (L) and M is the weight (g) of the adsorbent.

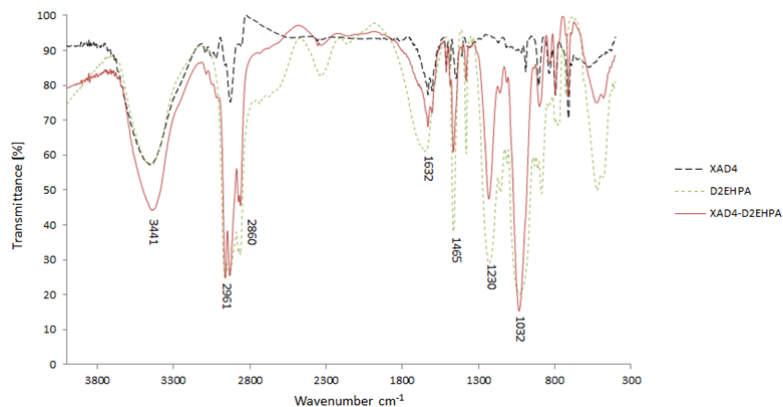


Fig. 2 FT-IR spectra of pure XAD-4, D2EHPA and XAD-4 impregnated with D2EHPA

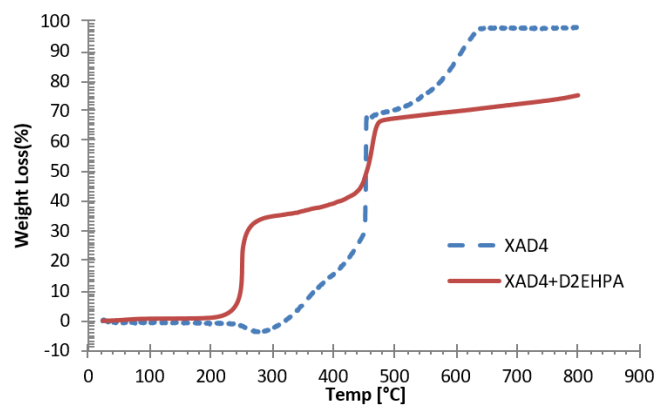


Fig. 3 Thermograms of XAD-4 resin and XAD-4 impregnated with D2EHPA

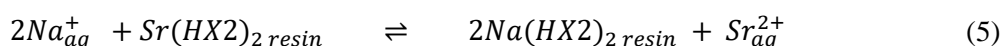
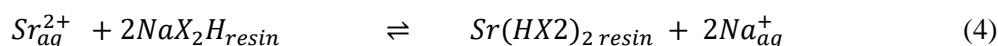
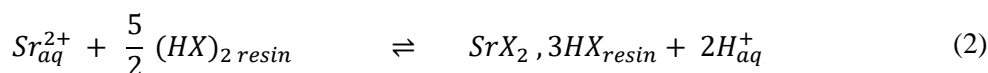
3. Results and discussion

3.1 Characterization of impregnated resin

The FT-IR spectra of pure XAD-4, D2EHPA and XAD-4 impregnated with D2EHPA are presented in Fig. 2. The characteristic bands of D2EHPA are P=O, P-O-C, P-O-H and O-H, and these bands are given at 1230, 1032, 1632 and 3441 cm^{-1} respectively (Krishan Kant *et al.*, 2013). Other bands are less important and correspond with aliphatic and aromatic bonds related to styrene divinyl benzene. Fig. 3 shows the thermograms of pure impregnated Amberlite XAD-4 and D2EHPA up to 800°C. The weight loss for the impregnated resin in the range of 230-260°C (about 30%) can be attributed to either destruction or evaporation of D2EHPA and residue remaining after 700-800°C (about 20%) is related to the decomposition products of D2EHPA and formation of phosphorous oxides. The weight loss at temperature 460°C relates to the start of the resin degradation.

3.2 Effect of pH on Sr (II) adsorption

We used 0.1 M HCL and 0.1 M NaOH solutions for adjusting pH. As can be seen in Fig. 4(a), the Sr(II) uptake is strongly pH-dependent. The maximum uptake occurs at pH 8.0 with 94% recovery. This behavior of the impregnated resin can be attributed to the more stable complexes of Sr (II) ions with D2EHPA at alkaline pH. The following mechanism can be written for Sr(II) adsorption onto impregnated resin



where $(\text{HX})_2$ refers to the dimeric species of D2EHPA. It should be noted that the dimerization/polymerization of D2EHPA molecule is one of the limiting factors during M^{n+} -D2EHPA complexation. The earlier study shows that with increasing D2EHPA concentration, polymerization increases namely, the rate of complex formation decreases with increasing D2EHPA concentration (Peppard *et al.* 1985). When D2EHPA concentration reaches to the highest value in the pores of the resin (after evaporation of the solvent), dimerization factor will be more important in the decrease of rate of Sr (II)-D2EHPA formation at lower pH. As Eq. 2 shows, the formation of Sr(II)-D2EHPA complex involves the association of five molecules of D2EHPA with one Sr (II) ion (Ashraf Chaudry *et al.* 1994). It can be anticipated that the reaction rate is very slow in neutral aqueous solutions because of the formation of relatively large complex ($\text{SrX}_2 \cdot 3\text{HX}$, Eq. 2). Our preliminary experiments showed that Sr(II)-D2EHPA species cannot be formed in dilute acid solutions. For instance, the adsorption of Sr (II) ions reaches to less than one percent at pH=1. Fig. 4(a) shows the variation of adsorption versus pH in the range of 3 to 11. By adding alkali to the solution containing impregnated resin, H^+ ions are consumed and sodium salt of D2EHPA is formed and dimer species are decomposed to monomers (Eq. (3)). Under these

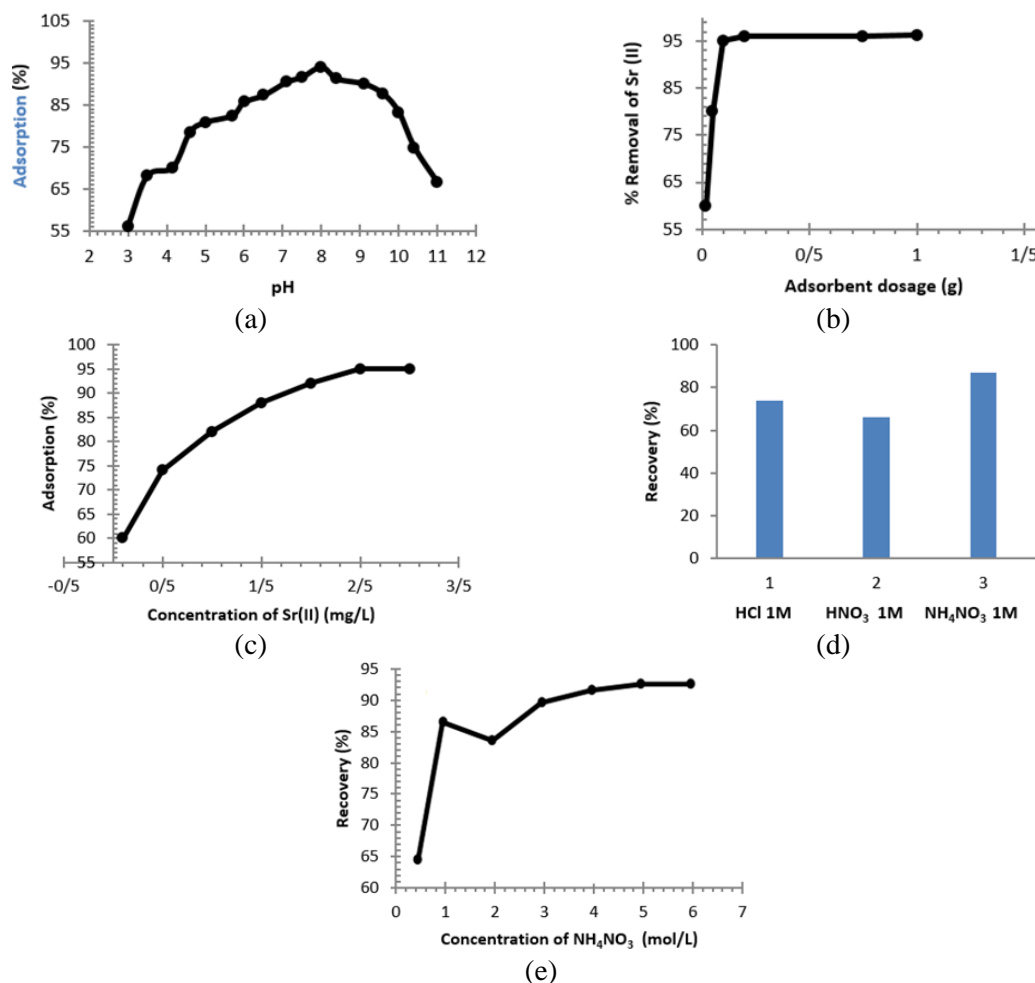


Fig. 4 (a) Effect of pH on Sr removal onto D2EHPA–XAD-4 resin, (b) Effect of adsorbent dose on Sr removal, (c) Effect of initial concentration on Sr removal at optimal conditions, (d) Effect of various solvents on the recovery of Sr (II) ion with 10 ml of eluant and (e) Recovery of Sr (II) ions under optimal ammonium nitrate condition

conditions, Sr (II) ions are easily complexed with D2EHPA molecules and the Sr (II) adsorption reaches to its highest values (Eq. (4)). When excess alkali is added, Sr (II)-D2EHPA complexes are decomposed by the rapid acid-base reaction of NaOH and D2EHPA, and as a result Sr(II) adsorption decreases to its lowest values at pH=11(Eq. (5)).

3.3 Effect of dose of impregnated resin

A series of experiments was carried out in which adsorbent dosage was varied in the range of 0.02-1.0 g. (Fig. 4(b)). The uptake of Sr (II) increases from 60.0 to 96.2 % with increasing the impregnated resin namely; there would be greater sites for metal ions adsorption under higher dosage of the impregnated resin. The best amount of adsorbent for removal of Sr (II) obtained was

0.25g. Increasing the amount of adsorbent did not show any significant changes on adsorption process. This can be due to overlapping of adsorption sites relevant to overfilling of adsorbent particles. Considering this fact, 0.2 g of adsorbent was chosen for further experiments.

3.4 Impact of initial concentration of Sr (II)

According to the various parameters affecting on the Sr (II) adsorption, initial ionic concentration which can provide a high concentration driving force between liquid and solid phase and decreasing the mass transfer resistance is of great importance. The impact of initial concentration in the range of 0.1 to 3 mg/L was studied (pH 8.0 and the adsorbent dose of 0.2 g, stirring speed of 180 rpm, contact time of 360 min and temperature of 25°C). The maximum adsorption occurs in the initial concentration of 2.5 mg/L (Fig. 4(c)).

3.5 Desorption study

Desorption of Sr (II) was investigated with 10 ml solutions of 1M HCl, 1M HNO₃ and 1M NH₄NO₃ (at pH=8). A considerable amount of Sr (II) ions was desorbed by applying these solutions. As shown in Fig. 4(d), better result was obtained with 1M NH₄NO₃, and desorption efficiency obtained was 87%, while for HCl and HNO₃ were 74% and 66% respectively. The significant differences between ammonium nitrate desorption and the other two aforementioned acids can be attributed to the formation of D2EHPA-NH₄ salt in alkaline region. More experiments with the same volume of 5M NH₄NO₃ showed a Sr (II) recovery of 93% (Fig. 4(e)).

3.6 Effect of contact time on adsorption-desorption

The effect of contact time on Sr (II) uptake was studied in the range of 5-120 minutes. As can be seen from Fig. 5(a), strontium uptake reaches the equilibrium about 30 min. Under this condition, the adsorption capacity of Sr (II) was found to be 0.45 mg/g. Similarly, Sr(II) elution can be fulfilled with 10 mL of 5 mol/L NH₄NO₃. The desorbed Sr (II) ions can be calculated using the difference between adsorbed Sr(II) and the final concentration of Sr(II). After charging the D2EHPA-XAD-4 resin with 5 mg/L Sr (II) solution, desorption was almost fast and reached to the equilibrium within 30 to 60 min (Fig. 5(a)). We repeated the adsorption-desorption process to determine the regeneration and desorption efficiency of the D2EHPA-XAD-4. The Sr(II) capacity decreased from 0.5 to about 0.041 mg/g at the fourth adsorption step after repeated loading with 5 mg/L solution and 30 min incubation period.

3.7 Equilibrium isotherms of adsorption

Equilibrium isotherm of adsorption shows the mathematical relationship between the amount of adsorbate and the equilibrium concentration of ion in the solution at a constant temperature. To survey the adsorption isotherms, 0.2 g of resin beads was mixed with 20 mL solution and stirred for 4 hrs under various concentrations of Sr (II) at different temperatures of 20, 30 and 40°C. As Fig. 5(b) shows, the capacity of D2EHPA-XAD-4 increases with increasing the initial concentration of the Sr (II) ions. Under such condition, the Sr (II) capacity amounted to 0.45 mg/g with initial concentration of 20 mg/L. Isotherm curves were estimated using different models (Tables 1 and 2). Fig. 6 suggests The Jossens, Weber-van Vliet and Fritz-Schlunder isotherms at various temperatures.

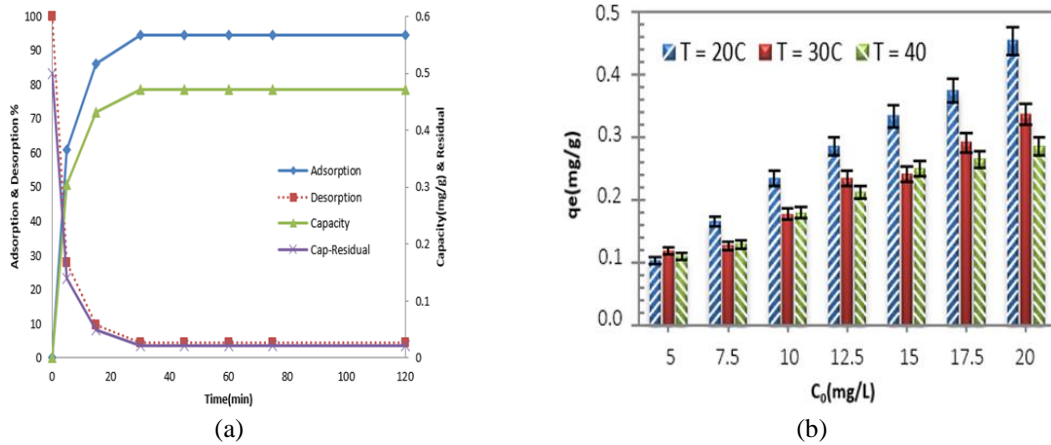


Fig. 5 (a) Adsorption and desorption of Sr (II) ions as the function of time and (b) Effect of initial concentration and temperature on the uptake of Sr (II) ions

Table 1 Types of adsorption isotherms and their equations

| Model | Parameter | Equation |
|------------------|-----------|---|
| Langmuir | 2 | $q_e = \frac{q_{ml}K_l C_e}{1 + K_l C_e}$ |
| Freundlich | 2 | $q_e = K_f C_e^{1/n_f}$ |
| Temkin | 2 | $q_e = B_t \ln(A_t C_e)$ |
| Elovich | 2 | $\frac{q_e}{q_{me}} = K_e C_e \exp(-\frac{q_e}{q_m})$ |
| Toth | 2 | $q_e = \frac{K_t C_e}{(K_t + C_e)^{1/n_t}}$ |
| Redlich-Peterson | 3 | $q_e = \frac{A_r C_e}{1 + B_r C_e^{n_r}}$ |
| Generalized | 3 | $q_e = \frac{q_{mg} C_e^{ng}}{K_g + C_e^{ng}}$ |
| Jossense | 3 | $C_e = \frac{q_e}{K_j} \exp(n_j q_e^{m_j})$ |
| Radke-prausnitz | 3 | $q_e = \frac{q_{mrp} K_{rp} C_e}{(1 + K_{rp} C_e)^{n_{rp}}}$ |
| Fritz-Schlunder | 4 | $q_e = \frac{q_{mfs} K_{fs1} C_e^{n_{fs}}}{1 + K_{fs2} C_e^{m_{fs}}}$ |
| Weber-Van Vliet | 4 | $C_e = K_w q_e^{(n_w q_e^{m_w} + l_w)}$ |

q_e : equilibrium capacity, C_e : adsorbed equilibrium concentration, q_m : maximum capacity, K, A, B : equilibrium constants, m, n, l : power constants

Table 2 Isotherm parameters obtained using different non-linear models*at different temperatures

| isotherm | Temperatures(°C) | Coefficients | | R ² |
|----------|------------------|--------------|--------|----------------|
| | | qml | kl | |
| Langmuir | 40 | 0.6270 | 0.0489 | 0.9798 |
| | 30 | 1.2879 | 0.0202 | 0.9521 |
| | 20 | 16.20 | 0.0018 | 0.9894 |

Table 2 Continued

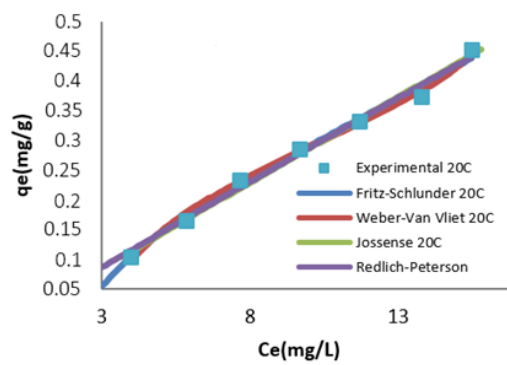
| isotherm | Temperatures(°C) | Coefficients | | | R ² | |
|------------------|------------------|-----------------------|--------------------------|---------|----------------|--------|
| | | nf | kf | | | |
| Freundlich | 40 | 1.4843 | 0.0428 | | 0.9755 | |
| | 30 | 1.2337 | 0.0333 | | 0.9591 | |
| | 20 | 1.1013 | 0.0296 | | 0.9836 | |
| Temkin | | At | Bt | | | |
| | 40 | 0.5394 | 0.1252 | | 0.9642 | |
| | 30 | 0.4716 | 0.1476 | | 0.8938 | |
| Elovich | | qme | ke | | | |
| | 40 | 1.34×10^4 | 1.41×10^{-6} | | 0.9020 | |
| | 30 | 8.62×10^3 | 2.4075×10^{-6} | | 0.9460 | |
| Redlich-Peterson | | Ar | Br | nr | | |
| | 40 | 0.0264 | 0.0089 | 1.4793 | 0.9805 | |
| | 30 | 7.51×10^{10} | 2.2533×10^{12} | 0.1894 | 0.9591 | |
| Toth | | Kt1 | Kt2 | nt | | |
| | 40 | 1.3×10^{-5} | 1.5813 | -0.1161 | 0.9745 | |
| | 30 | 0.1200 | 6.9075×10^{-19} | -23.61 | 0.9704 | |
| Generalized | | qmg | kg | ng | | |
| | 40 | 0.6168 | 20.3503 | 1.0084 | 0.9798 | |
| | 30 | 1.87×10^{10} | 5.6157×10^{11} | 0.8106 | 0.9591 | |
| jossens | | Kj | nj | mj | | |
| | 40 | 0.0225 | 1229 | 6.4840 | 0.9872 | |
| | 30 | 777.77 | 10.78 | 0.0172 | 0.9636 | |
| radke-prausnitz | | qmrp | krp | nrp | | |
| | 40 | 280.08 | 1.016×10^{-4} | 311.56 | 0.9811 | |
| | 30 | 8.11×10^{-4} | 97.99 | 0.1896 | 0.9591 | |
| weber-van vliet | | kw | nw | mw | lw | |
| | 40 | 71.1446 | -2.26×10^{-8} | 16.6723 | 1.2498 | 0.9913 |
| | 30 | 37.82 | -21.955 | 0.0103 | 22.46 | 0.9664 |
| fritz-schlunder | | Kfs1 | Kfs2 | nfs | mfs | |
| | 40 | 0.0354 | 1×10^{-10} | 0.7668 | 7.3533 | 0.9867 |

Table 2 Continued

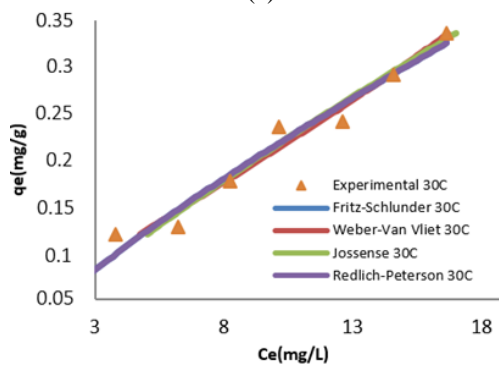
| isotherm | Temperatures(°C) | Coefficients | | | | R ² |
|-----------------|------------------|-----------------------|--------|--------|------------------------|----------------|
| fritz-schlunder | | Kfs1 | Kfs2 | nfs | mfs | |
| | 30 | 0.2698 | 7.0996 | 0.8106 | -6.57×10 ⁻⁹ | 0.9591 |
| | 20 | 2.72×10 ⁻⁴ | 0.0080 | 5.6467 | 4.7143 | 0.9917 |

*The sum of square of the average squares of the errors(ERAV) was selected for curve fitting because its R-

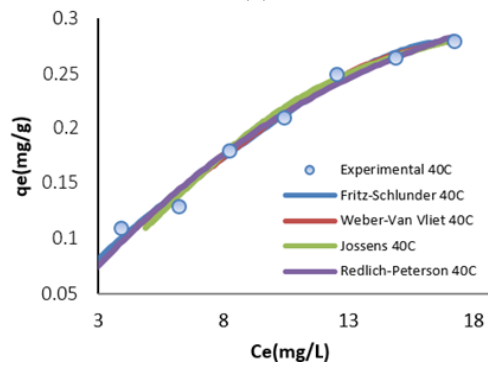
square is lowest and its expression as follows: $f = \sqrt{\frac{1}{n} \sum_{i=1}^n (y_{exp} - y_{cal})^2}$



(a)



(b)



(c)

Fig. 6 Isotherm curves obtained by the best non-linear modeling at various temperatures

3.8 Adsorption kinetic models

To find out the mechanism of the adsorption, we examined the pseudo-first-order and pseudo second-order equations. For simple kinetic analysis, we can apply the pseudo-first-order equation as follows

$$dq_t/dt = k_1 (q_e - q_t) \quad (6)$$

where k_1 is the rate constant of pseudo-first-order adsorption and q_e presents the adsorption capacity (i.e. the adsorption agrees to monolayer coverage). After definite integration by applying the initial conditions $t=0$ to t and $q_t=0$ to q_t , Eq. (6) becomes

$$\ln (q_e - q_t) = \ln(q_e) - k_1.t \quad (7)$$

where q_e and q_t are Sr (II) ions adsorbed (mg.g^{-1}) at equilibrium and at time t , k_1 is the constant (min^{-1}). The plot of $\ln (q_e - q_t)$ versus t gives a straight line for the pseudo-first-order adsorption kinetics (Fig. 7(a)).

The pseudo-first-order rate constant (k_1) results from the slope of the straight line ($k_1 = -0.1972$). The q_e value can be estimated from the intercept ($q_{e1} = 0.459$). The pseudo-second-order model is as follows

$$dq_t/dt = k_2 (q_e - q_t)^2 \quad (8)$$

where k_2 is the rate constant of pseudo-second-order adsorption. With integration of Eq. (8) and applying the initial conditions, we have

$$t/q_t = (1/k_2)q_e + (1/q_e)t \quad (9)$$

The pseudo-second-order plots for Sr(II) ions at pH 8 is shown in (Fig 7b). The pseudo-second-order rate constant k_2 , and q_{e2} were calculated from the intercept ($k_2 = 0.381986$) and from the slope ($q_{e2} = 0.465875$) respectively. Considering the correlation coefficients obtained for the pseudo-first-order ($R^2 = 0.9945$) and pseudo-second-order ($R^2 = 0.9997$), it seems likely that pseudo-second-order mechanism dominates the sorption kinetics.

Here, entropy (ΔS°) (KJ/ mol, K), enthalpy (ΔH°) (kJ/ mol) and free energy (ΔG°) (kJ/ mol) can be estimated using the following equations

$$K_0 = C_{\text{solid}}/C_{\text{liquid}} \quad (10)$$

$$\Delta G^\circ = -RT \ln K_0 \quad (11)$$

$$\ln K_0 = \Delta S^\circ / R - \Delta H^\circ / RT \quad (12)$$

where K_0 , C_{solid} , C_{liquid} , T and R are the equilibrium constant, solid phase concentration at equilibrium (mg/L), liquid phase concentration at equilibrium (mg/L), temperature in Kelvin, and gas constant (8.314 J/mol, K) respectively. By plotting the graph of $\ln(K_0)$ versus $1/T$ (Fig. 7(c)), the values ΔH° and ΔS° are estimated from the slopes and intercepts. As shown in Table 3, the negative ΔG° value suggests Sr (II) adsorption onto the D2EHPA-XAD-4 resin is thermodynamically possible and spontaneous. The negative ΔH° value suggests the exothermic nature of adsorption. The positive value of ΔS° shows a randomness increase at the solid-solution interface. Physical adsorption occurs if free energy ΔG° is about -20 to -40 kJ/mol and if ΔG° is to be greater than -40 kJ/mol, chemical adsorption is dominant mechanism. In the case of chemical

adsorption, a coordinate bond is formed due to charge sharing or transfers from the solid-phase surface to a metal ion. The ΔG° value obtained in this study for the Sr (II) ions is < -9 kJ/mol, suggesting that physical adsorption was the dominant mechanism of adsorption.

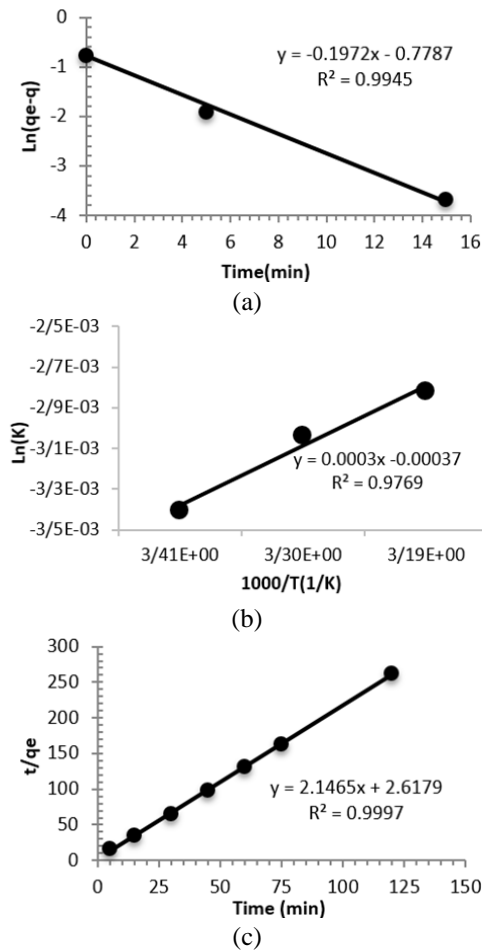


Fig. 7 (a) Pseudo-first-order kinetics for the removal of Sr (II) ions by D2EHPA impregnated XAD-4 resin at different concentrations, (b) Pseudo-second-order kinetics for the removal of Sr (II) ions by D2EHPA impregnated XAD-4 resin at different concentrations and (c) $\ln(K_c)$ vs. $1/T$ for adsorption of Sr (II) ions on D₂EHPA –XAD-4 resin

Table 3 Thermodynamic parameters for the adsorption of Sr (II) ions onto D₂EHPA –XAD-4 resin

| C ₀ (mg/L) | dG(kJ/mol) | | | dH(kJ/mol) | dS(KJ/mol.K) |
|-----------------------|------------|---------|---------|------------|--------------|
| | T=20 °C | T=30 °C | T=40 °C | | |
| 5 | -8.04 | -8.78 | -8.77 | 2.54 | -0.0365 |
| 7.5 | -8.23 | -7.70 | -7.80 | -14.43 | 0.0215 |
| 10 | -8.42 | -7.81 | -8.12 | -12.66 | 0.0150 |
| 12.5 | -8.33 | -7.99 | -7.90 | -14.59 | 0.0215 |

Table 3 Continued

| C ₀ (mg/L) | dG(kJ/mol) | | | dH(kJ/mol) | dS(KJ/mol.K) |
|-----------------------|---------------------|---------------------|---------------------|------------|--------------|
| | T=20 ^o C | T=30 ^o C | T=40 ^o C | | |
| 15 | -8.24 | -7.51 | -7.88 | -13.33 | 0.0180 |
| 17.5 | -8.12 | -7.62 | -7.58 | -15.96 | 0.0270 |
| 20 | -8.30 | -7.65 | -7.34 | -22.32 | 0.0480 |

Table 4 Effect of interfering ions on the adsorption of Sr (II) ions

| Interfering Ion | A (mg/L) | %L | %E | D |
|-----------------|----------|------|----|-----|
| - | 4.7 | 0 | 94 | 9.4 |
| Cd+2 | 4.0 | 14.9 | 80 | 8.0 |
| Ni+2 | 3.75 | 20.2 | 75 | 7.5 |
| Ca+2 | 3.0 | 36.2 | 60 | 6.0 |
| Mg+2 | 2.5 | 48.8 | 50 | 5.0 |
| Fe+2 | 3.75 | 20.2 | 75 | 7.5 |
| Ba+2 | 3.5 | 25.5 | 70 | 7.0 |
| Al+3 | 3.9 | 17.0 | 78 | 7.8 |
| Mixed Above | 2.0 | 57.4 | 40 | 4.0 |

A: Amount of adsorbed Sr (II) (mg/L), L: Loss adsorption (%), E: extraction percentage (%)

And D: distribution ratio

Table 5 Results of Sr (II) recovery after spiking in various water samples

| Sample | Spiked(mg/L) | Found(mg/L) | ^a Recovery% + RSD% |
|-------------|--------------|-------------|-------------------------------|
| Tap Water | 0.0 | 0.14 | - |
| | 0.2 | 0.34 | 100 ± 2.9 |
| | 0.4 | 0.55 | 101.8 ± 3.7 |
| Well Water | 0.0 | 3.13 | - |
| | 0.2 | 3.33 | 100 ± 3.0 |
| | 0.4 | 3.47 | 98.3 ± 3.7 |
| River Water | 0.0 | 6.7 | - |
| | 0.2 | 7.07 | 102.5 ± 2.9 |
| | 0.4 | 7.2 | 101.4 ± 2.8 |

3.9 Effect of foreign ions on adsorption of Sr(II)

The effect of various foreign ions (5 mg/L) on the uptake of Sr (II) ions (concentration 5 mg/L) was investigated and extraction percentage (E%) from the following equations was calculated

$$Q = (C_0 - C_e) V / W \quad (13)$$

$$E = C_e / C_0 \quad (14)$$

$$D = E V / W \quad (15)$$

$$L = C_e^{\text{No-ion}} - C_e / C_e^{\text{No-ion}} \quad (16)$$

where Q is the resin capacity (mg/g), C_o and C_e stand for the initial and equilibrium concentration (µg/ mL), W, V and E% are the mass of the resin (0.2 g), the volume of solution (0.02L) and the extraction percentage. As is shown in Table 4, the interfering ions have negligible effect on Sr (II) uptake.

3.10 Analysis of real samples

To examine the ability of the impregnated resin under real conditions, adsorption of Sr (II) in various water samples was investigated and the results are given in table 5. It should be noted that before starting these experiments, the pH of all water samples was adjusted to 8. The following formula was used for recovery percent

$$\text{Recovery}_{(N+1)} \% = \frac{C_{\text{Found}(N+1)}}{C_{\text{Spiked}(N+1)} + C_{\text{Found}(N)}} \times 100 \quad (17)$$

4. Conclusions

The presented method is simple and rapid for the preconcentration of Sr (II) ions from aqueous solutions. The impregnated resin used has an acceptable adsorption capacity toward the Sr (II) ion. The results of kinetics models confirm the pseudo-second order can be applicable for the reaction rate of Sr(II) ions with the impregnated resin. The uptake of strontium ions was found to be 94.0% at optimal pH. Also, the results show that ammonium nitrate is a suitable eluant to desorb Sr (II) ions from the surface of the resin with 93 percent recovery. As a result, it can potentially be used to estimate Sr (II) ions quantitatively in different real samples.

Acknowledgements

The authors would like to acknowledge all those who aided in this work, and the nuclear science and technology research institute for financial and technical supports.

References

- Bilgin, B., Atun, G. and Keçeli, G. (2001), "Adsorption of strontium on illite", *J. Radioanal. Nucl. Chem.*, **250**(2), 323-328.
- Cakir, P., Inan, S. and Altas, Y. (2014), "Investigation of strontium and uranium sorption onto zirconium-antimony oxide/polyacrylonitrile (Zr-Sb oxide/PAN) composite using experimental design", *J. Hazard. Mater.*, **271**, 108-119.
- Chaudry, M.A. and Ahmad, I. (1994), "Extraction and stripping study strontium ions across D2EHPA-TBP-Kerosene oil based supported liquid membrane", *J. Radioanal. Nucl. Chem.*, **185**(2), 369-385.

- Chen, J.H., Chen, W.R., Gau, Y.Y. and Lin, C.H. (2003), "The preparation of di(2-ethylhexyl) phosphoric acid modified Amberlite 200 and its application in the separation of metal ions from sulfuric acid solution", *React. Funct. Polym.*, **56**(3), 175-188.
- Chen, P.Y. (2007), "The assessment of removing strontium and cesium cations from aqueous solutions based on the combined methods of ionic liquid extraction and electrodeposition", *Electrochimica Acta*, **52**(17), 5484-5492.
- Ding, S.D., Yang, T., Liu, N. and Zhang, L. (2010), "Extraction behavior of strontium from nitric acid solution with N,N,N',N'-tetraisobutyl diglycolamide", *J. Iran. Chem. Soc.*, **7**, 545-553
- Greve, K., Nielsen, E. and Ladefoged, O. (2007), "Evaluation of health hazards by exposure to strontium in drinking water", *Toxicol. Lett.*, **172**(S210).
- Grynpas, M.D., Hamilton, E., Cheung, R., Tsouderos, Y., Deloffre, P., Hott, M. and Marie, P.J. (1996), "Strontium increases vertebral bone volume in rats at a low dose that does not induce detectable mineralization defect", *Bone*, **18**(3), 253-259.
- Hafizi, M., Abolghasemi, H., Moradi, M. and Milani, S.A. (2011), "Strontium adsorption from sulfuric acid solution by Dowex 50W-X resins", *Chin. J. Chem. Eng.*, **19**(2), 267-272.
- Heilgeist, M. (2000), "Use of extraction chromatography, ion chromatography and liquid scintillation spectrometry for rapid determination of strontium-89 and strontium-90 in food in cases of increased release of radionuclides", *J. Radioanal. Nucl. Chem.*, **245**(2), 249-254.
- Jeong, S.K. and Ju, C.S. (2002), "Extraction of strontium ion from sea water by contained liquid membrane permeator", *Kor. J. Chem. Eng.*, **19**(1), 93-98.
- Kocherginsky, N.M., Zhang, Y.K. and Stucki, J.W. (2002), "D2EHPA based strontium removal from strongly alkaline nuclear waste", *Desalination*, **144**(1-3), 267-272.
- Makrlík, E., Van'ura, P., Selucký, P. and Spíchal, Z.K. (2010), "Solvent extraction of calcium and strontium into nitrobenzene by using a synergistic mixture of hydrogen dicarbollycobaltate and 2,6-(diphenylphosphino) pyridine dioxide", *Acta Chimica Slovenica*, **58**, 860-865.
- Mazhar, M. (2009), "Potassium iron (III) hexacyanoferrate (II) supported on polymethylmethacrylate ion-exchanger for removal of strontium (II)", *J. Radioanal. Nucl. Chem.*, **281**(3), 393-403.
- Nielsen, S.P. (2004), "The biological role of strontium", *Bone*, **35**(2), 583-588.
- Peppard, D.F., Ferraro, J.R. and Mason, G.W. (1985), "Hydrogen bonding in organophosphoric acids", *J. Inorg. Nucl. Chem.*, **7**(3), 231-244.
- Pröhl, G., Ehlken, S., Fiedler, I., Kirchner, G., Klemm, E. and Zibold, G. (2006), "Ecological half-lives of ⁹⁰Sr and ¹³⁷Cs in terrestrial and aquatic ecosystems", *J. Environ. Radioact.*, **91**(1-2), 41-72
- Puziy, A.M. (1998), "Cesium and strontium exchange by the framework potassium titanium silicate K₃HTi₄O₄(SiO₄)₃·4H₂O", *J. Radioanal. Nucl. Chem.*, **237**(1-2), 73-79.
- Raut, D.R., Mohapatra, P.K. and Manchanda, V.K. (2012), "A highly efficient supported liquid membrane system for selective strontium separation leading to radioactive waste remediation", *J. Membr. Sci.*, **390**, 76-83.
- Schulz, W.W., Mendel, J.E. and Richardson, G.L. (1963), "Solvent extraction recovery and purification of strontium-90", *Ind. Eng. Chem. Proc. Des. Dev.*, **2**(2)134-140.
- Schutz, W.W. (1968), *Effects of some Synergistic and Antagonistic Agents on HDEHP Extraction of Strontium* (No. BNWL--759), Pacific Northwest Lab, Battelle-Northwest, Richland, Washington, D.C., U.S.A.
- Singh, K.K., Pathak, S.K., Kumar, M., Mahtele, A.K., Tripathi, S.C. and Bajaj, P.N. (2013), "Study of uranium sorption using D2EHPA-impregnated polymeric beads", *J. Appl. Polym. Sci.*, 3355-3364
- Sivaiah, M.V., Venkatesan, K.A., Krishna, R.M., Sasidhar, P. and Murthy, G.S. (2005), "Ion exchange properties of strontium on in situ precipitated polyantimonic acid in amberlite XAD-7", *Sep. Purif. Technol.*, **44**(1), 1-9.
- Solecki, J. and Michalik, S. (2006), "Studies of ⁸⁵Sr adsorption on grain fractions of soil", *J. Radioanal. Nucl. Chem.*, **267**(2), 271-278.
- Tripathi, A., Medvedev, D.G., Nyman, M. and Clearfield, A. (2003), "Clearfield Selectivity for Cs and Sr in Nb-substituted titanosilicate with sitinakite topology", *J. Solid State Chem.*, **175**(1), 72-83.

- Ye, X., Liu, T., Li, Q., Liu, H. and Wu, Z. (2008), "Comparison of strontium and calcium adsorption onto composite magnetic particles derived from Fe₃O₄ and bis(trimethoxysilylpropyl)amine", *Colloid. Surface. A Physicochem. Eng. Asp.*, **330**(1), 21-27.
- Zhang, L., Zhou, J., Zhou, D. and Tang, Y. (1999), "Adsorption of cadmium and strontium on cellulose/alginate ion-exchange membrane", *J. Membr. Sci.*, **162**(1-2), 103-109.

CC